

UNIVERSIDADE ESTADUAL DE CAMPINAS  
SISTEMA DE BIBLIOTECAS DA UNICAMP  
REPOSITÓRIO DA PRODUÇÃO CIENTÍFICA E INTELLECTUAL DA UNICAMP

**Versão do arquivo anexado / Version of attached file:**

Versão do Editor / Published Version

**Mais informações no site da editora / Further information on publisher's website:**

[https://www.epj-](https://www.epj-conferences.org/articles/epjconf/abs/2023/09/epjconf_uhecr2023_05011/epjconf_uhecr2023_05011.html)

[conferences.org/articles/epjconf/abs/2023/09/epjconf\\_uhecr2023\\_05011/epjconf\\_uhecr2023\\_05011.html](https://www.epj-conferences.org/articles/epjconf/abs/2023/09/epjconf_uhecr2023_05011/epjconf_uhecr2023_05011.html)

**DOI: 10.1051/epjconf/202328305011**

**Direitos autorais / Publisher's copyright statement:**

©2023 by EDP Sciences. All rights reserved.

DIRETORIA DE TRATAMENTO DA INFORMAÇÃO

Cidade Universitária Zeferino Vaz Barão Geraldo

CEP 13083-970 – Campinas SP

Fone: (19) 3521-6493

<http://www.repositorio.unicamp.br>

# Search for upward-going showers with the Pierre Auger Observatory

Vladimír Novotný<sup>1</sup> for the Pierre Auger Collaboration<sup>2,\*</sup>

<sup>1</sup>Institute of Particle and Nuclear Physics, Faculty of Mathematics and Physics, Charles University, V Holešovičkách 2, 180 00 Prague 8, Czech Republic

<sup>2</sup>Full author list: [http://www.auger.org/archive/authors\\_2022\\_10.html](http://www.auger.org/archive/authors_2022_10.html)

**Abstract.** Motivated by the ANITA report of pulses compatible with upward-going extensive air showers, we present a recent search for such showers using the Pierre Auger Observatory. The dataset, registered using the fluorescence detector of the Observatory, is scanned to identify showers ascending from the ground. Consistent with the exit angles reported from the first and third ANITA flights, we focus on shower geometries that are incompatible with Standard Model interactions of neutrinos in the Earth. We present the effective area of the Observatory to generic upward-going showers as a function of shower energy and altitude. This can be used to constrain predictions based on physics beyond Standard Model and the upgoing-shower interpretation of the ANITA results. To demonstrate the method, we calculate limits to the production rate of tau leptons near the ground emerging under a range of exit angles.

## 1 Introduction

The Pierre Auger Observatory [1], located near Malargüe, Argentina was built to investigate ultra-high energy cosmic rays (UHECRs). Nevertheless, it is also capable of measuring upward-going (UG) extensive air showers (EASs) that could be created by other particles than UHECRs. In this contribution, we search for EASs that would emerge from the ground with zenith angle ( $\theta$ ) above  $110^\circ$ . To this end, we utilize the fluorescence detector (FD) of the Observatory that is composed of 24 telescopes at four sites covering elevations up to  $30^\circ$ , and three High-Elevation Auger Telescopes (HEAT) looking between  $30^\circ$  and  $60^\circ$  in elevation.

Our search is motivated by ANITA report of radio pulses compatible with upward-going extensive air showers [2] and our choice of investigated zenith angles comply with these findings. It is worth noting that presence of UG EASs with that large  $\theta$  implies phenomena beyond the Standard Model of particle physics, because such showers would be inconsistent with interactions of neutrinos in the Earth and current limits on neutrino flux provided by the Auger Observatory [3].

## 2 Analysis

Showers ascending from the ground can be distinguished in the FD from downward-going (DG) EASs using the trigger time information from individual FD pixels together with their pointing. On top of that, we utilize an approximately universal longitudinal shape of EASs that must be compatible with calculated profile of the energy deposited in the atmosphere [4]. The later is especially

important to assess the geometry of showers detected only in one FD station for which the time and pointing information is not sufficient for short tracks.

After the cleaning of the dataset from lasers used to monitor the atmosphere, Section 2.1, we estimate the number of background events, Section 2.2, calculate the FD exposure to UG events, Section 2.3, and, finally, unblind the data and assess the number of candidate events, Section 2.4.

### 2.1 Laser cleaning

To efficiently filter events coming from monitoring lasers of the Observatory, occurring occasionally in undefined times due to technical malfunctions, a burnt dataset (10 % of the full sample) was unblinded in advance and not used in the final analysis. The distribution of impact points of events in the burnt sample before and after the laser cleaning is shown in Fig. 1. The apparent lines occur due to misreconstruction of laser events that are shot from the two laser facilities in the centre of the array and from LIDARs located at four FD sites. Thus, the residual laser events are rejected based on the azimuth of the direction of normal to the shower-detector plane and on specific frequencies of laser shots.

### 2.2 Background

In the case that a shower is detected only in one FD station, i.e. we use a monocular reconstruction to calculate the shower axis, the shower can be wrongly reconstructed. As a consequence, ordinary downward-going EASs can mimic UG signal. A shower falling behind the FD telescope produces an image on the FD camera that is moving

\*e-mail: [spokespersons@auger.org](mailto:spokespersons@auger.org)

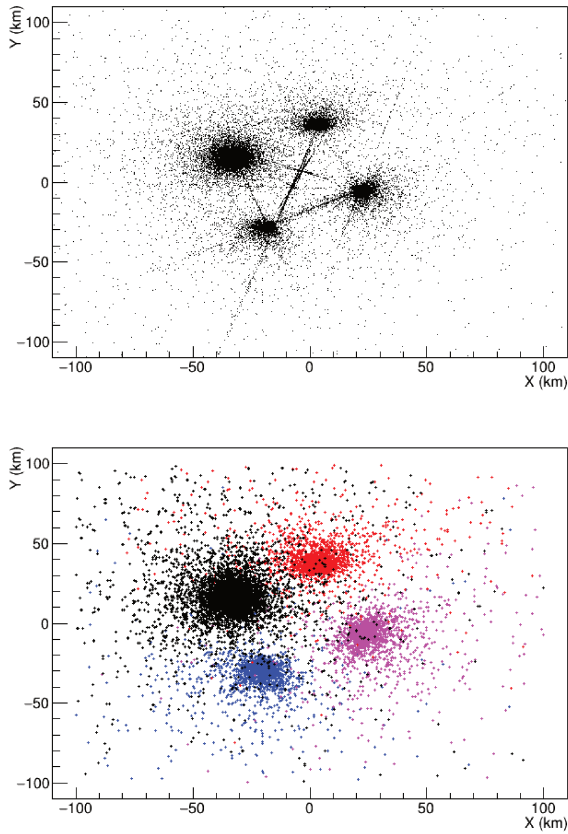


**Figure 1.** Distribution of shower cores in the burnt dataset before and after the laser cleaning process in the top and bottom panel, respectively. Apparent lines in the upper panel correspond to the misreconstructed laser events, and colours in the bottom panel represent FD sites that detected individual showers.

from low to high elevations, which is also consistent with the UG shower emerging in front of the telescope. This is visualised in Fig. 2.

To identify as many of events falling behind the telescope as possible, we apply a specific data cleaning that uses maximum likelihood values  $L_{up}$  and  $L_{down}$  coming from competing DG and UG geometry reconstructions, respectively. The decisive quantity that selects UG candidates is

$$l = \frac{\arctan\left(-2 \log\left(L_{down}/\max\left(L_{up}, L_{down}\right)\right)/50\right)}{\pi/2}, \quad (1)$$

which is cut, after optimization using simulations [5], above 0.55 to select signal.

After the cleaning procedure, a background of  $0.45 \pm 0.18$  events is expected in the full data sample. The distributions of the  $l$  quantity, Eq. (1), are shown in Fig. 3 for the burnt dataset, background simulations, and signal simulations. The correspondence between the burnt sample and the background distributions is a non-trivial result that comes from the precise knowledge of the detector and energy spectrum of UHECRs provided by the Pierre Auger Observatory.

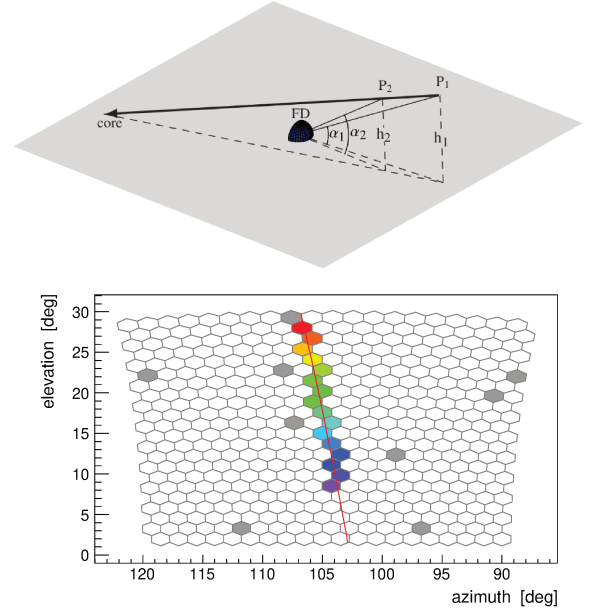


**Figure 2.** Geometry of a downward-going EAS with an impact point behind the field of view of an FD telescope (top panel). An image of such a shower moves in the field of view from bottom (magenta - former) to up (red - later) as marked by colours of triggered pixels (bottom panel). Gray pixels correspond to random triggers. The red line represents a projection of the shower axis.

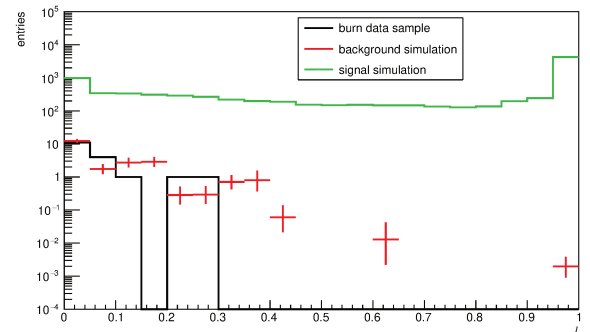


**Figure 3.** Distributions of the  $l$  quantity in the burnt dataset (black), background simulations (red), and signal simulations (green). Background simulations are weighted to the UHECR flux measured by the Auger Observatory and normalized to 10 % of the data. The normalization of the signal simulations is arbitrary.

## 2.3 Exposure

Extensive Monte Carlo (MC) simulations were produced to estimate the FD exposure to UG EASs. Protons, chosen as primaries, were thrown in geometries that correspond to an isotropic emergence from the ground with the height of the first interaction ( $H_{fi}$ ) sampled equally between 0 and 9 km. This range is limited by the field of view (FoV) of the FD telescopes. Quantities used to define the injection of particles into the MC simulations are visualized in Fig. 4.

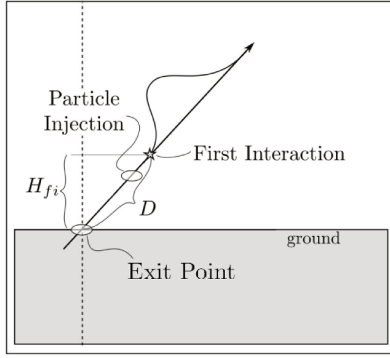


**Figure 4.** Parameters used in the simulation of UG EASs. Height of the first interaction  $H_{fi}$ , and the distance between the particle exit point from the ground and the first interaction  $D$  are shown.

After the application of the selection criteria, briefly described in Section 2.2, to the MC simulated showers, we evaluate selection efficiency and exposure in individual energy– $H_{fi}$  bins. In Fig. 5, we present the double-differential exposure of the FD to UG EASs w.r.t.  $H_{fi}$  and calorimetric energy of showers ( $E_{cal}$ ). It allows one to test any type of exotic model of production of EASs, provided that the distribution of emergence of showers with altitude is predicted. Effective areas restricted to zenith angle bins of  $\theta \in [110^\circ, 124.2^\circ]$ ,  $\theta \in [124.2^\circ, 141.3^\circ]$ , and  $\theta \in [141.3^\circ, 180^\circ]$  were also calculated [5].

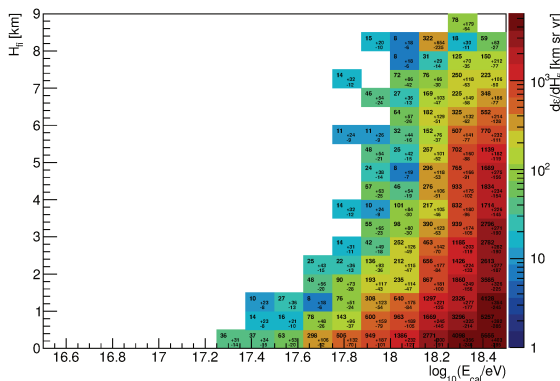


**Figure 5.** The double-differential exposure of the FD to UG EASs. An isotropic emergence of events for  $\theta \in [110^\circ, 180^\circ]$  is assumed.

## 2.4 Candidates

After unblinding, 1 event has been observed to pass all the selection criteria in the full data sample. This is in line with the background expectation. Thus, we place upper limits on the integral flux of UG showers at 95 % confidence level, assuming two different spectral indices  $\gamma = 1, 2$

$$F_{\gamma=1}^{95\%} = 3.6 \cdot 10^{-20} \text{ cm}^{-2} \text{ sr}^{-1} \text{ s}^{-1}, \quad (2)$$

$$F_{\gamma=2}^{95\%} = 8.5 \cdot 10^{-20} \text{ cm}^{-2} \text{ sr}^{-1} \text{ s}^{-1}. \quad (3)$$

These limits are valid for any UG EASs with  $E_{cal}$  above  $10^{17.5}$  eV.

The double-differential exposure table shown in Section 2.3 can be used also to place differential limits in individual energy bins, and even place limits using specific scenario of the production of UG showers. This is illustrated in Section 3.

## 3 Upper limits on the flux of $\tau$ leptons

Having the previous results in hand, upper limits on a particular scenario of the EAS production from  $\tau$  leptons can be set [6]. We assume a flux of  $\tau$ s in the energy range of  $E_{0,\tau} \in [10^{16.5} \text{ eV}, 10^{20} \text{ eV}]$ .

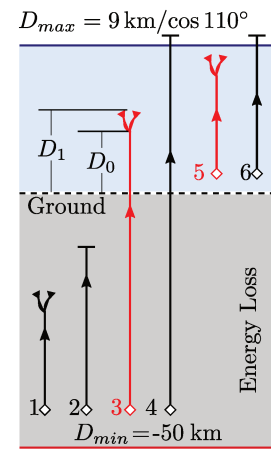


**Figure 6.** Possible outcomes of the  $\tau$  simulations in NuTauSim. The height  $H_{fi}$  in Fig. 4 corresponds to the distance  $D_1$ , where the decay products of the  $\tau$  interact.

Using the MC simulations in NuTauSim [7], we investigated the  $\tau$  propagation in the Earth assuming their isotropic production in the distance range of  $D \in [-50 \text{ km}, 26.3 \text{ km}]$  around the ground plane. According to the sketch in Fig. 6, only in cases 3 and 5, for which the  $\tau$  decay appears in the FD-observable part of the atmosphere, we simulated the decay of  $\tau$  in TAUOLA [8]. We obtained the distribution of  $\tau$ -decay induced EASs within the FoV of the FD shown in the top panel of Fig. 7.

The distribution of  $\tau$  induced EASs is then folded with the double-differential exposure of the FD from Fig. 5 to get the number of events per height bin that would trigger the FD, given in the bottom panel of Fig. 7. It is further integrated in height for each energy bin.

After the calorimetric energy of  $\tau$  EASs ( $E_{sh}$ ) is tracked back to  $E_{0,\tau}$ , we place differential upper limits on the emergence of  $\tau$  leptons near the ground shown in Fig. 8. Because each  $E_{0,\tau}$  contributes to several  $E_{sh}$ , due to the energy distribution of  $\tau$ -daughter particles, we assume two spectral indices of the  $\tau$  flux,  $\gamma = 1, 2$ , to calculate the limits.

These limits hold irrespectively of the underlying scenario of the  $\tau$  production.

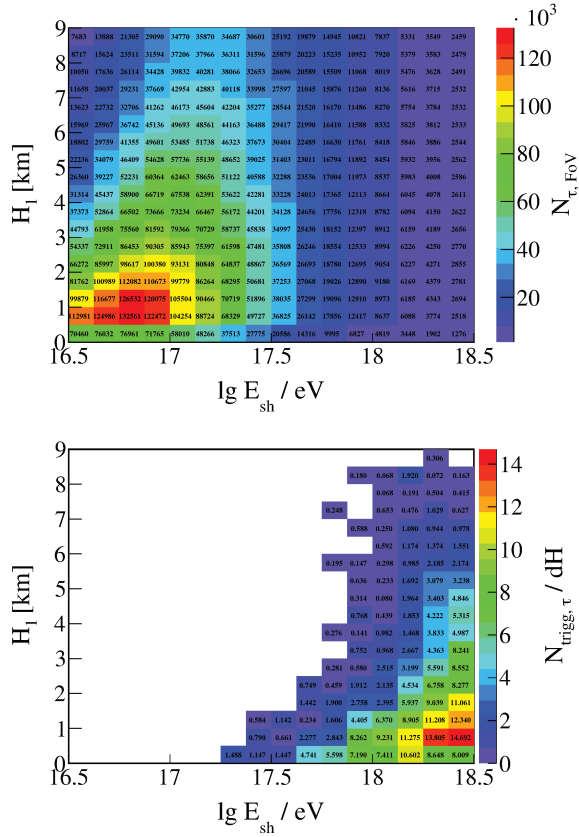


**Figure 7.** Distribution of MC-generated  $\tau$ -decay induced EASs within the FoV of the FD (top panel) and corresponding number of FD-triggered events per height bin (bottom panel). The height  $H_1$  corresponds to the distance  $D_1$  in Fig. 6 and coincides with  $H_{fi}$ .

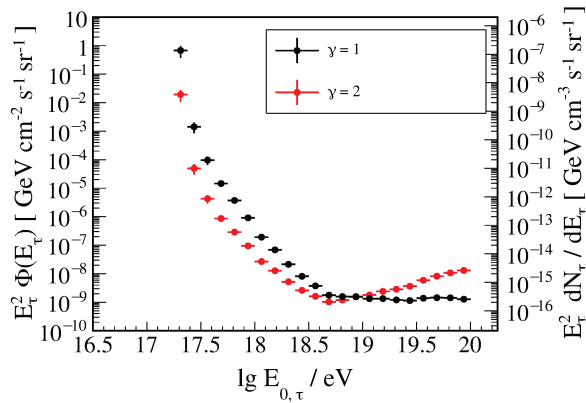


**Figure 8.** Differential upper limits on the isotropic emergence of  $\tau$  leptons near the ground at 95 % confidence level. The left axis corresponds to the flux of  $\tau$ -leptons created within 50 km of path length below the Earth's surface, and the right scale shows the limits on the rate of  $\tau$ s generated per unit volume, energy, and solid angle. Two indicated spectral indices of the  $\tau$  flux are assumed.

## 4 Conclusions

The data of 14 years of operation of the fluorescence detector of the Pierre Auger Observatory have been searched for upward-going extensive air showers with zenith angles between  $110^\circ$  and  $180^\circ$ . One candidate event has been found, which is consistent with the background expectation of  $\sim 0.5$  events, coming from wrongly reconstructed downward-going cosmic-ray showers. Integral upper limits on the flux of upward-going showers were determined for two spectral indices,  $\gamma = 1, 2$ , used in the calculation of an average exposure. The double-differential exposure of the fluorescence detector was presented, and was applied to derive upper limits on the  $\tau$  lepton emergence near the ground.

## Acknowledgement

This work was supported by the Czech Ministry of Education, Youth and Sports grant LTT18004.

## References

- [1] A. Aab et al. (Pierre Auger), Nucl. Instrum. Meth. A **798**, 172 (2015)
- [2] P.W. Gorham et al. (ANITA), Phys. Rev. Lett. **121**, 161102 (2018)
- [3] L. Perrone et al. (Pierre Auger), these proceedings (2022)
- [4] V. Novotny et al. (Pierre Auger), PoS **ICRC2019**, 374 (2021)
- [5] M. Mastrodicasa et al. (Pierre Auger), PoS **ICRC2021**, 1140 (2021)
- [6] I.A. Caracas et al. (Pierre Auger), PoS **ICRC2021**, 1145 (2021)
- [7] J. Alvarez-Muñiz et al., Phys. Rev. D **97**, 023021 (2018), [Erratum: Phys.Rev.D 99, 069902 (2019)]
- [8] M. Chruszcz, T. Przedzinski, Z. Was, J. Zaremba, Comput. Phys. Commun. **232**, 220 (2018)